

Electronic Supplementary Information

Engineering a molecular-sieving architecture on PIL- functionalized UiO-66-NH₂ membranes toward CO₂/N₂ separation

Liangmei Luo, Yingjie Chang, Yutong Liao, Yanqing Wang* and Qi Li*

Department of Materials Science, School of Chemistry and Chemical Engineering,
Nantong University, Nantong 226019 Jiangsu, P. R. China

Corresponding author: Dr. Qi Li, E-mail: zhuiqiuzhizhuo@163.com

Experimental Section

2.1. Chemicals and Reagents

Polyethylene terephthalate (PET, thickness: 22 μm ; diameter: 4.5 cm; pore size: 200 nm) membrane was obtained from Beijing (China) SFLB Technology Co., Ltd.. 1,4-Dibromobutane ($\geq 98.0\%$), Zirconium tetrachloride (ZrCl_4 , $\geq 99.5\%$), 2-amino-1,4-benzene dicarboxylic acid (NH_2 -BDC), and 1-vinyl-3-butylimidazolium tetrafluoroborate ([VBIM][BF₄]) were purchased from Aladdin Reagent (Shanghai) Co., Ltd. All other auxiliary reagents were of analytical grade and used without further purification, such as dimethylformamide (DMF) (98.0%) obtained from Sinopharm Chemical Reagent Co., Ltd. Deionized water was used for all experiments.

2.2. *In situ* growth of UiO-66-NH_2 on PET surface

In brief, a piece of PET was firstly soaked in 3 M HNO_3 solution for 12 h, then washed with deionized water until the pH of filtrate to 7. Subsequently, ZrCl_4 (28.80 mg, 0.12 mmol) was dissolved in acetic acid at 80 $^\circ\text{C}$ (1.3 mL) for 1 h. After cooling to room temperature, DMF (15 mL) and NH_2 -BDC (22 mg, 0.12 mmol) were put into a 50 mL round flask and ultrasonic until dissolved, followed by the addition of a piece of PET membrane and soaking for 2 h. Finally, the solution was transferred into a Teflon-lined stainless steel autoclave and kept in an oven for 24 h at 120 $^\circ\text{C}$ under static conditions. When the reaction temperature cooled to room temperature, the PET membrane was washed with water for several times and dried under vacuum at 60 $^\circ\text{C}$ for 24 h. The as-prepared membrane is denoted PET/ UiO-66-NH_2 .

2.3. Synthesis of PET/ UiO-66-NH_2 @PIL membrane

First, a 5 mL solution of the ionic liquid monomer [VBIM][BF₄] with a concentration of 0.03 mol/L was prepared. Add 2 mg of N,N'-methylenebisacrylamide crosslinker and stir at room temperature until fully dissolved. Subsequently, add 50 mg of the photoinitiator (1-hydroxycyclohexyl phenyl ketone) and stir magnetically. Finally, uniformly coat the resulting ionic liquid-containing solution onto the surface of a PET film and perform photopolymerization under 360 nm UV light for 1 hour to obtain the composite membrane. The sample dried in air at 80 °C, and the product was denoted as PET/UiO-66-NH₂@PIL.

2.4. Characterization

The crystal structures were analyzed by powder X-ray diffraction (XRD) using a Philips X'Pert PRO diffractometer with Cu K α radiation ($\lambda=1.5406$ Å). Morphological characterization was performed using field-emission scanning electron microscopy (FESEM; Hitachi S-4700) and high-resolution transmission electron microscopy (HRTEM; FEI Tecnai G2 F20) equipped with an energy-dispersive X-ray spectroscopy (EDS) detector. Gas sorption properties were evaluated through N₂ adsorption-desorption measurements at 77 K and CO₂ adsorption isotherms at 298 K using a Micromeritics ASAP 2020 Plus HD88 analyzer. Prior to analysis, all samples were thermally activated at 120°C under vacuum for 24 h. Pore size distributions were derived from the adsorption branch data using the Barrett-Joyner-Halenda (BJH) model. Structural verification of ionic liquids was achieved through ¹H nuclear magnetic resonance (NMR) spectroscopy recorded at 303 K on a Bruker DRX-400 spectrometer operating at 600 MHz.

2.5. Calculations of gas separation factor

The mixed gas separation factor (SF, α_{ij}) is defined by following Eq 1:

$$\alpha_{ij} = \frac{y_i / y_j}{x_i / x_j} \quad (1)$$

Where y_i and y_j , x_i and x_j are the molar ratios of component i and j in the permeate and feed side, respectively.

2.6. Vacuum gas sorption test

Prior to adsorption measurements, all samples underwent thermal pretreatment involving vacuum degassing at 120 °C for 6 h to remove physisorbed contaminants. The activated samples were maintained under vacuum before introducing CO₂ gas into the system. Precise control of relative pressure (P/P_0) was achieved through a programmed sequence, systematically adjusting CO₂ partial pressure to target values (0.05, 0.2, 0.3, 0.5, 0.6, 0.8, 0.9, 0.95). Gravimetric adsorption data, including time-dependent mass variations, were continuously monitored using high-resolution microbalance instrumentation until equilibrium conditions were met (defined as mass stability within $\pm 0.01\%$ over 30 min).

2.7. Pseudo-second-order equation

$$\frac{t}{Q_t} = \frac{t}{Q_e} + \frac{1}{k_2 Q_e^2} \quad (2)$$

Where Q_t and Q_e refer to the equilibrium and maximum adsorption capacities of the adsorbent, respectively. t (min) represents contact time, and k_2 ($\text{g mg}^{-1} \text{min}^{-1}$) is the adsorption rate constant.

2.8. Gas permeation measurements

The gas permeation performance of PET/UiO-66-NH₂@PIL membrane was carried out using a Wicke-Kallenbach permeation apparatus.^{1,2} The permeation cell was securely sealed with O-rings, and the operating temperature was precisely set at 303 K. A gas mixture composed of CO₂ and N₂ in a volume ratio of 15:85 (v/v) was introduced to the feed side of the membrane, while maintaining the feed pressure at a constant 1 bar. Argon, flowing at a rate of 5 mL min⁻¹, was employed as the sweep gas. Once the system had achieved a stable state, the composition of the gas mixture on the permeate side was analyzed by a pre-calibrated gas chromatograph (GC, FULI 9790). The concentration of each gas component was continuously monitored until no further change was detected, guaranteeing the accuracy and reliability of the test results.

Gas permeance is determined according to the following Eq. (3):

$$P_i = \frac{N_i}{A\Delta P_i} \quad (3)$$

Where P_i is the permeance of component i (mol m⁻² s⁻¹ Pa⁻¹), N_i refers to the permeate rate of component i (mol s⁻¹), A is presented as effective membrane area (m²), and ΔP_i refers to the transmembrane pressure difference for component i (Pa). GPU represents the unit of gas permeance. (1 GPU = 3.35×10⁻¹⁰ mol m⁻² s⁻¹ Pa⁻¹ at STP).

2.9. Molecular dynamics simulation

We first constructed two model systems, PET/UiO-66-NH₂ and PIL/UiO-66-NH₂, in which both PET and PIL consist of polymers with ten repeating units, to evaluate

their interaction energies with UiO-66-NH₂ structures (Fig. S9a, b). Subsequently, a composite membrane system, PET-UIO-66-NH₂@PIL, was built to investigate CO₂ transport behavior (Fig. S9c). All simulations were performed using the LAMMPS package. Each system was first subjected to energy minimization using the conjugate gradient method, followed by molecular dynamics simulations in the NVT ensemble at 300 K. For the PET/UiO-66-NH₂ and PIL/UiO-66-NH₂ systems, 1000 ps simulations were conducted to analyze van der Waals and electrostatic interactions, as well as the interfacial interactions between the polymers and UiO-66-NH₂. A 10 ns simulation was carried out for the PET-UIO-66-NH₂@PIL composite membrane to investigate CO₂ transport behavior.

Synthesis route:

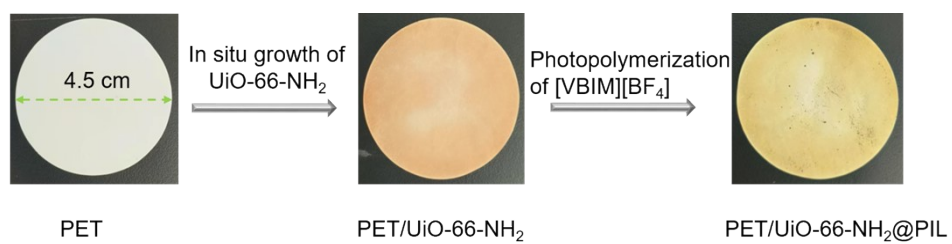


Figure S1. Synthesis route for the PET/UiO-66-NH₂@PIL membrane and corresponding digital photos.

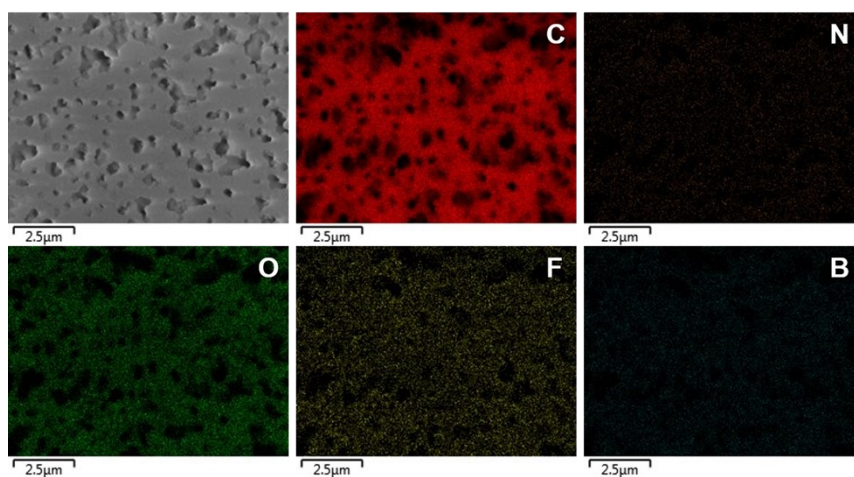


Figure S2. SEM image and corresponding elemental mapping of PET/UiO-66-NH₂@PIL.

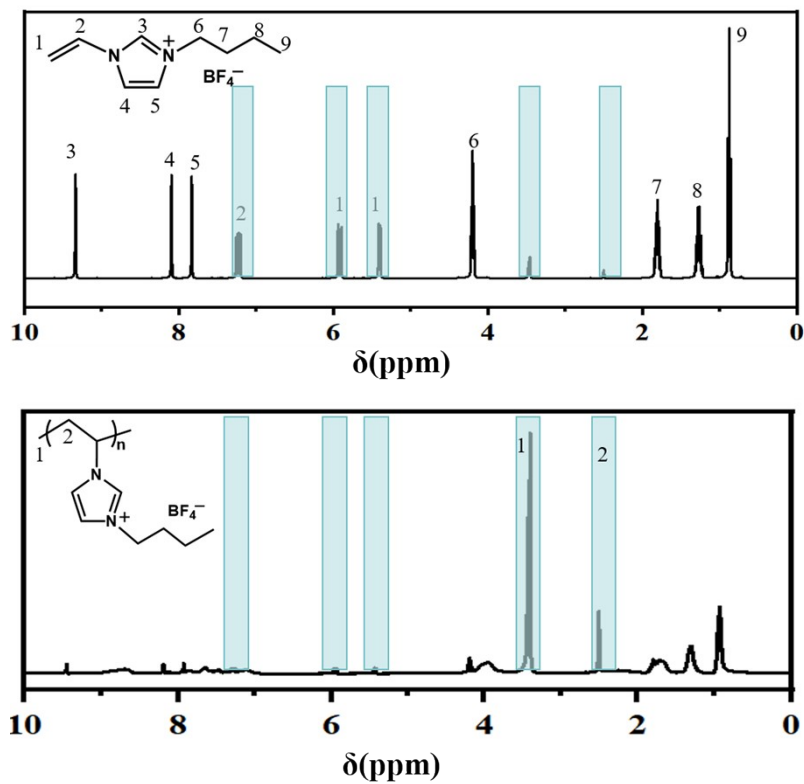


Figure S3. The ^1H NMR spectrum of PIL.

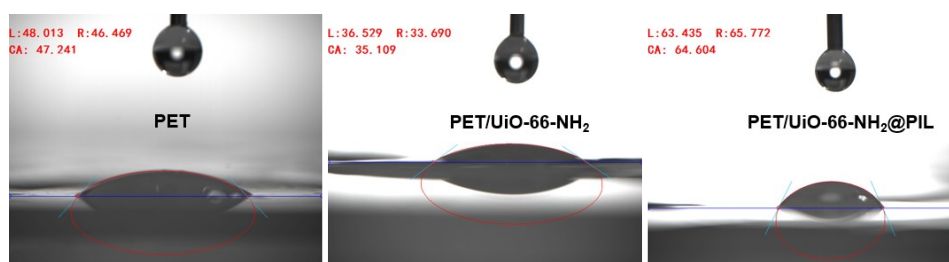


Figure S4. The water contact angle of PET, PET/UiO-66-NH₂, and PET/UiO-66-NH₂@PIL.

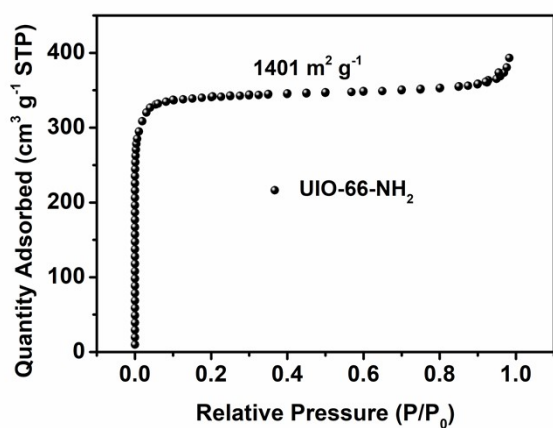


Figure S5. The BET surface area of UiO-66-NH₂.^[S1]

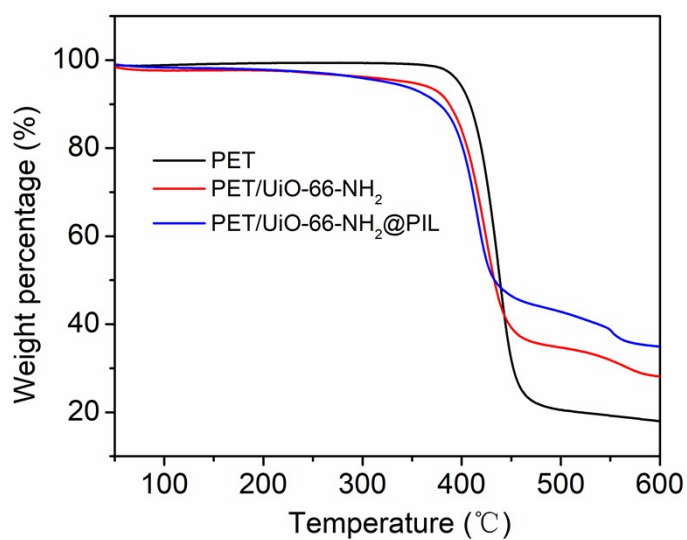


Figure S6. TGA curves of PET, PET/UiO-66-NH₂, and PET/UiO-66-NH₂@PIL under N₂ flow with a heating rate of 10 °C min⁻¹.

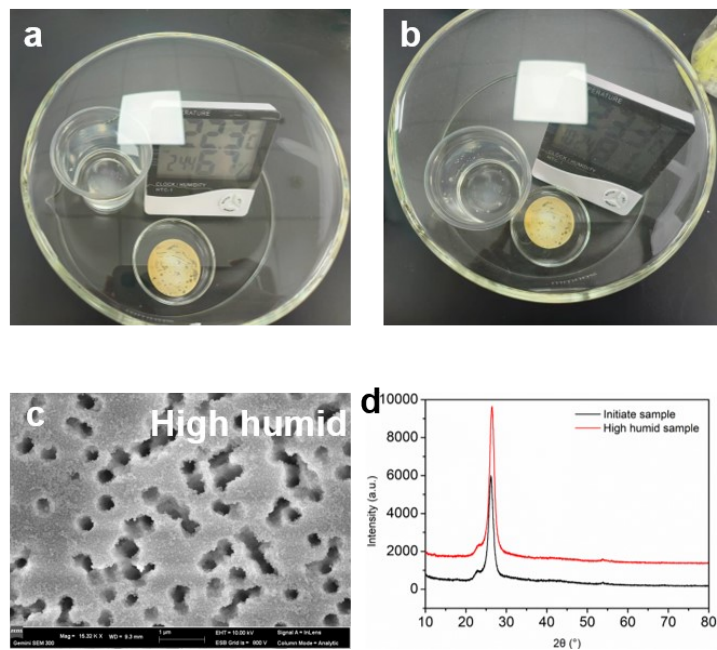


Figure S7. (a) Digital photographs of the original samples and (b) those stored in a high-humidity environment for 10 days. (c) SEM image and (d) XRD patterns of the PET/UiO-66-NH₂@PIL.

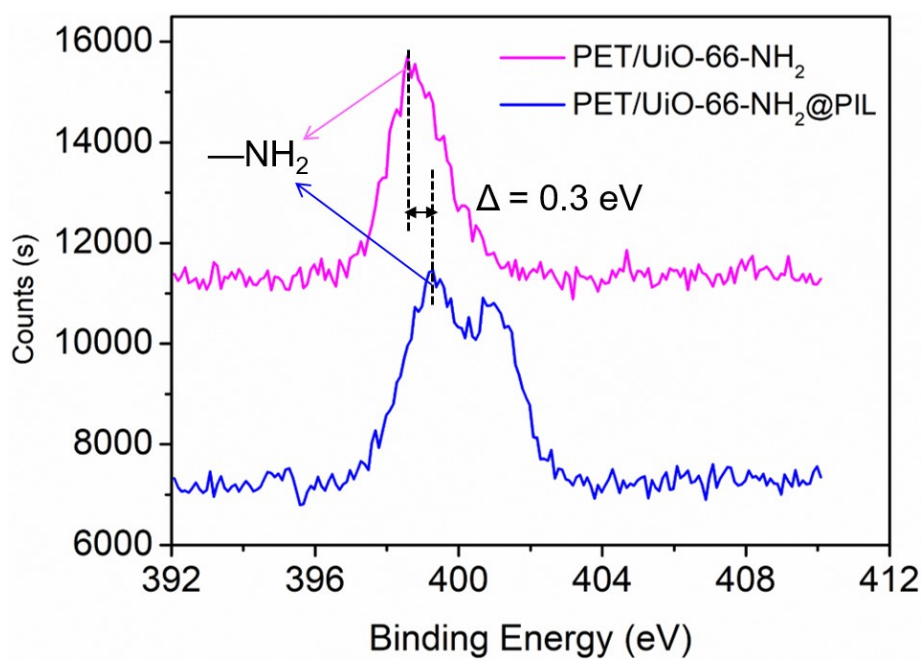


Figure S8. XPS spectra of PET/UiO-66-NH₂, and PET/UiO-66-NH₂@PIL.

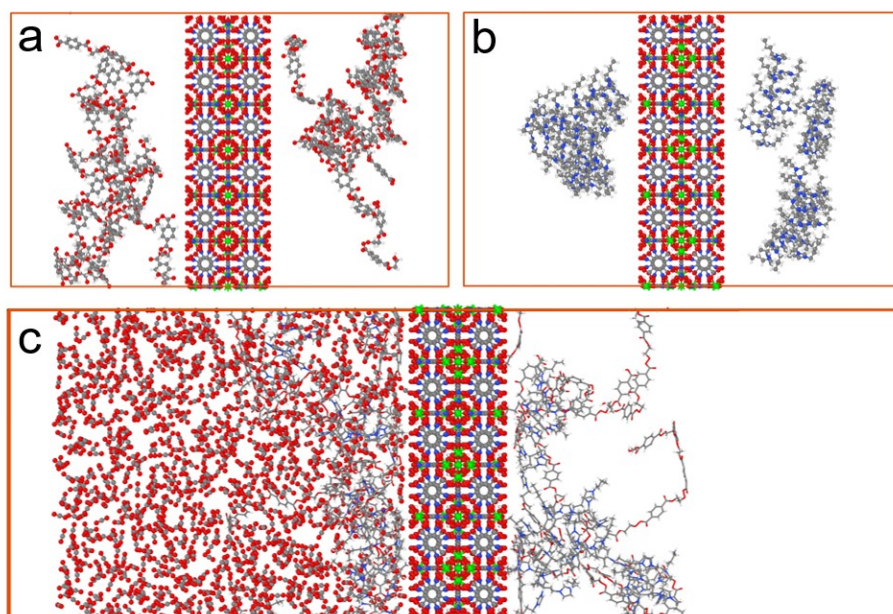


Figure S9. (a) The interaction energies of PET/UiO-66-NH₂ model, (b) PIL/UiO-66-NH₂ model and (c) PET/UiO-66-NH₂@PIL model.

References

S1. L. Luo, C. Xu, W. Shi, Q. Liu, Y. Ou-Yang, J. Qian, Y. Wang and Q. Li, *J. Phys. Chem. Lett.*, 2023, **14**, 8437–8443.